Development of an experimental database of EUV spectra from highly charged ions of medium to high Z elements in the Large Helical Device plasmas

Received: Added at production | Revised: Added at production | Accepted: Added at production

DOI: xxx/xxxx

ARTICLE TYPE

Development of an experimental database of EUV spectra from highly charged ions of medium to high Z elements in the Large Helical Device plasmas

C. Suzuki*[1] | I. Murakami[1,2] | F. Koike[3] | T. Higashiguchi[4] | H. A. Sakaue[1] | N. Tamura[1] | S. Sudo[5] | G. O'Sullivan[6]

[1]National Institute for Fusion Science, Toki, Japan
[2]SOKENDAI (The Graduate University for Advanced Studies), Toki, Japan
[3]Sophia University, Tokyo, Japan
[4]Utsunomiya University, Utsunomiya, Japan
[5]Chubu University, Kasugai, Japan
[6]University College Dublin, Dublin, Ireland

Correspondence
*C. Suzuki, 322-6 Oroshi-cho, Toki 509-5292, Japan
Email: csuzuki@nifs.ac.jp

Abstract

We are developing an experimental database of extreme ultraviolet (EUV) spectra from highly charged ions using optically thin high-temperature plasmas produced in the Large Helical Device (LHD). Spectra from a variety of elements with atomic numbers ranging from 36 to 83 have been systematically recorded in the 1–20 nm range by a grazing incidence spectrometer. For higher Z elements from tin onward, discrete or quasicontinuum spectral features from n=4 (N-shell) ions are mainly observed depending upon the plasma temperature, which leads to some new experimental identifications of spectral lines. On the other hand, major emitters are n=3 (M-shell) ions for medium Z elements from krypton to ruthenium. The calculated wavelengths for $\Delta n \neq 0$ transitions agree well with the measurements and the calculated wavelengths are systematically shifted to shorter wavelengths for Δn=0 transitions associated with inner-subshell excited configurations.

KEYWORDS:
EUV spectra; LHD; high Z elements; lanthanides; UTA

1 | INTRODUCTION

Magnetically confined torus plasmas for fusion research (MCF plasmas) have unique features unattainable in other types of plasma sources: low opacity, high brightness, large volume and high temperature as high as several keV. These features of MCF plasmas with flexibly controllable plasma temperature enable us to observe relatively clear spectra without large absorption or broadening in a wide temperature range. In addition, MCF devices are often equipped with impurity injection systems as well as powerful diagnostic tools for the measurements of plasma parameters and emission spectra. Therefore, MCF plasmas can often be exploited as light sources for spectroscopic studies on a variety of elements of interest not only in fusion but also in astrophysics or plasma applications [1, 2, 3, 4].

In this article, we review some of the principal results obtained in the development of an experimental database of extreme ultraviolet (EUV) and soft X-ray spectra from highly charged ions of a wide range of medium to high-Z elements using the Large Helical Device (LHD) at the National Institute for Fusion Science (NIFS). A variety of elements with atomic numbers ranging from 36 (krypton) to 83 (bismuth) have already been injected in the LHD to extend the database. The systematic studies on Z dependence of the spectra measured in the LHD lead to scientifically meaningful outcomes including new identifications of spectral lines from lanthanide ions [5, 6, 7]. Some of the measured spectral features have been compared with calculated line strength distributions, which indicates systematic deviations between the measurement and the calculation in some cases associated with n=4–4 or 3–3 (Δn=0) transitions.

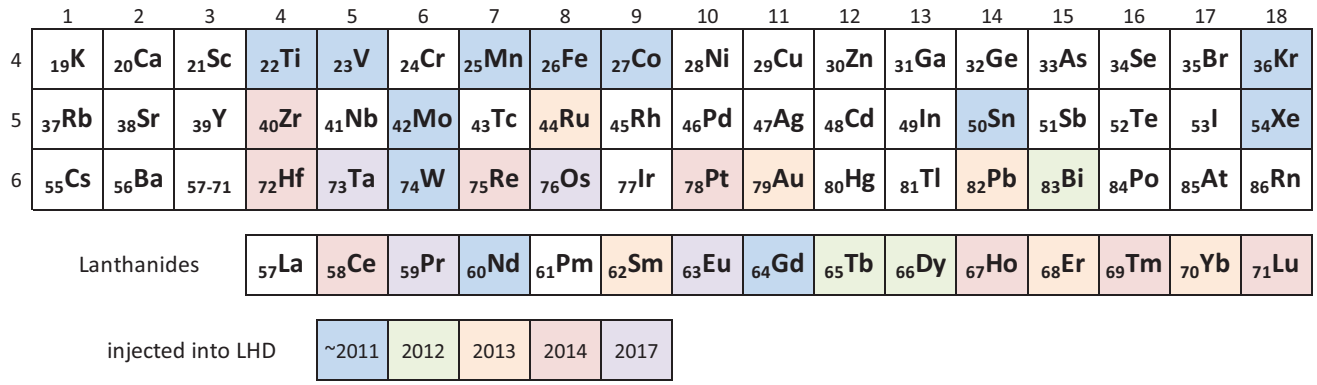

FIGURE 1 The 4th or higher period elements which have already been injected into LHD plasmas to date. The years of the first injection are indicated by different colors.

2 | EXPERIMENTAL

In the LHD experiments, small amounts of elements are introduced as impurities into high temperature (2–3 keV) and low density ((1–5)×10^{19} m^{-3}) hydrogen plasmas using gas puffing or a tracer encapsulated solid pellet (TESPEL) [8, 9]. Electron temperature and density profiles are directly measured by a Thomson scattering diagnostic system with excellent spatial and temporal resolutions [10, 11], which is suitable for studies on temperature dependence of EUV spectra. Time evolutions of the EUV and soft X-ray spectra are recorded in the 1–20 nm wavelength range by a 2 m grazing incidence spectrometer of Schwob-Fraenkel type [12] with a frame rate of 5–10 Hz. The 600 mm^{-1} groove density of the grating results in a wavelength resolution of about 0.01 nm. The plasma temperature rapidly drops due to a massive pellet injection or a reduction of heating power, which sometimes results in the formation of a "temperature hole" [5, 7, 13]. Therefore, we can acquire a variety of spectral data for a wide temperature range of approximately 0.3–3 keV in a single discharge.

A partial periodic table of the elements shown in Figure 1 indicates the 4th or higher period elements which have already been injected into LHD plasmas to date. Until now, more than 20 elements with atomic numbers higher than 36, including krypton, tin, tungsten, lanthanides and bismuth have been investigated in the LHD [5, 6]. Krypton and xenon are injected with gas puffing, while the other solid elements are injected with a TESPEL. The most frequently studied element among them is tungsten because of its importance in fusion research as a divertor material in ITER tokamak. Xenon, tin and gadolinium are important as candidate materials for light sources for the next-generation EUV nano-lithography, and the elements with atomic numbers of 78–83 may possibly be utilized for light sources in the "water window" wavelength region for high-contrast microscopy of biological samples [14, 15].

3 | SPECTRAL FEATURES OF N-SHELL IONS

For higher Z elements from tin (Z=50) onward, major emitters in the EUV and soft X-ray regions are ions with n=4 (N-shell) outermost electrons because the ionization energies of these ions correspond to the electron temperature ranges typically seen in the LHD plasmas. As discussed in a previous paper [13], the spectral features for these elements drastically change from discrete to quasicontinuum with decreasing electron temperature because of the change in ion abundance. The discrete and quasicontinuum spectral features are due to ions having 4s/4p and 4d/4f outermost electrons, respectively. The quasicontinuum feature, a so-called unresolved transition array (UTA) [16], is composed of a huge number of lines arising from complex energy level structures of ions with 4d/4f outermost electrons. Tungsten is the highest Z element for which the discrete feature could be observed so far in the LHD under the case of an electron temperature as high as 3 keV. The Z dependence of the UTA position observed in low temperature plasmas roughly follows the prediction of the quasi-Moseley's law [17] in the range of Z=50–83. The Z dependence of soft X-ray spectra from N-shell lanthanide ions with Z=60–70 has been systematically investigated, which leads to some new experimental identifications of spectral lines of neodymium, erbium, holmium and thulium ions [5, 6].

A UTA spectral feature in N-shell ions spectra is classified by whether the principal quantum number of the jumping electron changes or not in that transition; i.e., $\Delta n \neq 0$ or Δn=0. The center wavelength of the UTA moves to shorter wavelength with increasing ionic charge for n=4–5 or 4–6 transitions, while it stays in a similar wavelength region for n=4–4 transitions. For example, Figure 2 shows spectra of tungsten ions recorded in LHD plasmas with a peak temperature of 0.9 keV due to $\Delta n \neq 0$ and Δn=0 transitions which

appear in the 2–4 nm and 4.5–7 nm ranges, respectively. The line strength (weighted spontaneous transition probability) distributions for W^{22+}–W^{28+} calculated with the FAC (Flexible Atomic Code) [18] are also shown in Figure 2 by numerous vertical bars. The present calculation includes excited configurations $4d^{10}4f^{k-1}5l$, $4d^{10}4f^{k-1}6l$, and $4d^{9}4f^{k+1}$ for W^{22+}–W^{27+} (k=1–6), and $4d^{9}4f$, $4d^{9}5l$ and $4d^{9}6l$ for W^{28+}, where l denotes any possible symbols of angular momentum. All configuration interactions among these states are fully included in the FAC calculation.

The UTAs of n=4–5 or 4–6 transitions form a number of UTA peaks separated by each ion stage as shown in Figure 2 (a), while only a broadband UTA around 5 nm is observed for n=4–4 transitions as shown in Figure 2 (b). The calculated mean wavelengths of the UTAs for the 4f–5g and 4f–6g transitions of W^{22+}–W^{28+} ions are listed in Table 1, together with the measured wavelengths of the corresponding UTA peaks found in Figure 2 (a). Though some of the corresponding peaks are unclear in Figure 2 (a) due to weak intensity or blending, Figure 2 (a) and Table 1 demonstrate that the calculated wavelengths are in good agreement with the measurements for $\Delta n \neq 0$ transitions.

On the other hand, the calculated wavelengths are shifted to shorter wavelengths for Δn=0 (n=4–4) transitions as shown in Figure 2 (b). For example, the calculated and measured wavelengths of the singlet transition of Pd-like W^{28+} ($4d^{10}\ ^1S_0$ – $4d^9 4f\ ^1P_1$) are 4.790 nm and 4.895 nm, respectively. Though the FAC is a fully relativistic *ab initio* code based on the Dirac equation, these discrepancies are probably unavoidable due to the difficulties in the exact evaluation of the correlation energy among N-shell electrons in inner-subshell excited states such as $4d^9 4f^{k+1}$, as already discussed in the previous paper for lanthanide elements[6]. The assignment of a UTA peak for each ionic charge would be difficult for Δn=0 transitions because of the superposition of the UTAs in a similar wavelength region.

We have performed more realistic calculations of the transition wavelengths including as many configurations as possible in some cases using the HULLAC or GRASP92/RATIP code [6, 19]. In general, the GRASP92/RATIP calculation is time-consuming, but is expected to give better results because two electron non-local exchange integrals are treated as they are. Therefore, we have performed the GRASP92/RATIP calculations for the transition wavelengths of a few simple lanthanide ions to compare with the measurements [6]. Though small discrepancies still remains, the wavelengths calculated with the GRASP92/RATIP are closer to the measured ones for the Δn=0 transitions associated with inner-subshell excited configurations.

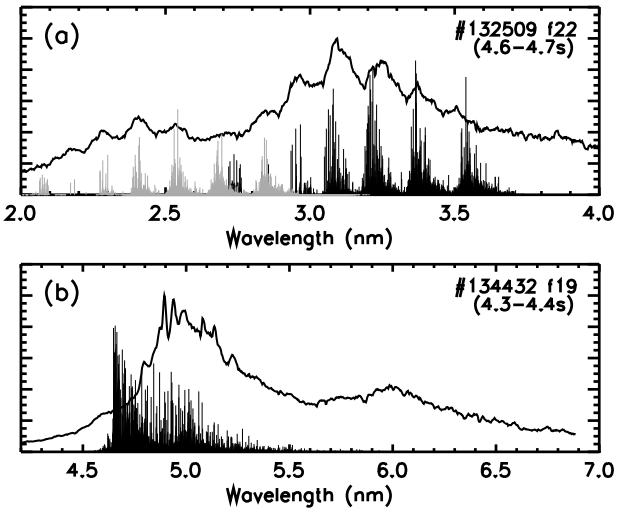

FIGURE 2 The measured spectra of tungsten ions for (a) $\Delta n \neq 0$ and (b) Δn=0 transitions observed in the LHD plasmas under a peak electron temperature of about 0.9 keV. The calculated line strengths are superposed with numerous vertical bars. Black and gray bars in (a) are due to 4f–5g and 4f–6g transitions, respectively, and all bars in (b) are due to $4d^{10}4f^k$–$4d^9 4f^{k+1}$ (k=0–6) transitions.

4 | SPECTRAL FEATURES OF M-SHELL IONS

We have also started a survey of EUV and soft X-ray spectra from ions with n=3 (M-shell) outermost electrons, which are dominant emitters for medium Z elements (roughly $30<Z<50$) under the temperature range in LHD plasmas. Spectra from M-shell ions tend to be less continuum-like in comparison with those from N-shell ions because of the smaller number of energy levels associated with the upper and lower configurations of M-shell ions. Although the survey of Z dependence is still incomplete, the measured spectra for even Z elements with atomic numbers between 36 and 44 are plotted in Figure 3 where the line strength distributions calculated with the FAC are superposed. The spectra for Δn=1 (n=3–4) and Δn=0 (n=3–3) transitions are shown in Figure 3 (a) and (b), respectively. The measurements for strontium, zirconium and ruthenium have not been completed yet in the LHD. The present line strength calculation includes all ion stages which have ground states with n=3 outermost electrons (from Na-like to Ni-like ions). In the calculation, all of the valence subshell excited configurations with n up to 5 are considered as well as inner subshell excited configurations such as $3s3p^{k+1}$ or $3s^2 3p^5 3d^{k+1}$.

The wavelengths of $\Delta n \neq 0$ transitions of M-shell ions also moves to shorter wavelengths with increasing ionic charge in a similar way to N-shell ions. This leads to a number of separate

TABLE 1 The calculated mean wavelengths ("Mean λ") of the UTAs for 4f–5g and 4f–6g transitions of W^{22+}–W^{28+} ions. The "Lines" column shows the number of lines in each UTA. The measured wavelengths of the corresponding UTA peaks found in Figure 2 (a) are listed in "LHD" column. The "unclear" means that the corresponding peak is unclear due to weak intensity or blending.

	4f–5g transition			4f–6g transiton		
		Wavelength (nm)			Wavelength (nm)	
Ion	Lines	Mean λ	LHD	Lines	Mean λ	LHD
W^{28+} (Pd-like)	152	2.742	(unclear)	151	2.081	(unclear)
W^{27+} (Ag-like)	3	2.846	2.85	3	2.179	2.17
W^{26+} (Cd-like)	123	2.967	2.96	125	2.292	2.28
W^{25+} (In-like)	2082	3.100	3.09	2097	2.416	2.41
W^{24+} (Sn-like)	16594	3.246	3.25	16827	2.552	2.54
W^{23+} (Sb-like)	72797	3.407	(unclear)	74116	2.703	(unclear)
W^{22+} (Te-like)	181418	3.588	(unclear)	193895	2.869	(unclear)

TABLE 2 The calculated mean wavelengths ("Mean λ") of the UTAs for 3d–4p and 3d–4f transitions of K^{8+}–Kr^{17+} ions. The "Lines" column shows the number of lines in each UTA. The measured wavelengths of the corresponding UTA peaks found in the top panel of Figure 3 (a) are listed in "LHD" column. The "unclear" means that the corresponding peak is unclear due to weak intensity or blending.

	3d–4p transition			3d–4f transition		
		Wavelength (nm)			Wavelength (nm)	
Ion	Lines	Mean λ	LHD	Lines	Mean λ	LHD
Kr^{17+} (K-like)	3	4.446	(unclear)	3	3.527	3.53
Kr^{16+} (Ca-like)	59	4.826	4.80, 4.85	79	3.737	3.71, 3.76
Kr^{15+} (Sc-like)	446	5.260	5.25	658	3.976	3.97
Kr^{14+} (Ti-like)	1536	5.760	5.71	2455	4.253	4.23
Kr^{13+} (V-like)	2814	6.343	6.31	4697	4.575	4.55
Kr^{12+} (Cr-like)	2864	7.030		4759	4.956	(unclear)
Kr^{11+} (Mn-like)	1605	7.851		2571	5.411	(unclear)
Kr^{10+} (Fe-like)	467	8.932		690	5.964	(unclear)
Kr^{9+} (Co-like)	57	10.030		81	6.643	(unclear)
Kr^{8+} (Ni-like)	3	11.497		3	7.499	

blocks of lines as shown in Figure 3 (a) in the 1.5–7 nm region where the series of the peaks due to 3d–4*l* and 3p–4*l* transitions are grouped in longer and shorter wavelength regions, respectively. Also, the measured structures for $\Delta n \neq 0$ transitions can be well explained by the calculations. For example, the calculated mean wavelengths of the UTAs for 3d–4p and 3d–4f transitions of krypton ions are listed in Table 2 to compare with the measured peak positions. On the other hand, lines due to the 3p–3d transitions appear in the 5.5–11 nm region as shown in Figure 3 (b). Again, the position of the Δn=0 transitions stays in a similar wavelength region regardless of ionic charge unlike n=3–4 transitions. It is also clearly seen that the calculated positions of the spectral features systematically shifts to shorter wavelengths from the measured ones.

5 | SUMMARY

We have systematically recorded a number of spectra from highly charged ions with atomic numbers ranging from 36 to 83 to develop an experimental database of EUV and soft X-ray spectra, exploiting unique features of the LHD plasmas. For N-shell ions, quasicontinuum UTA and discrete spectral

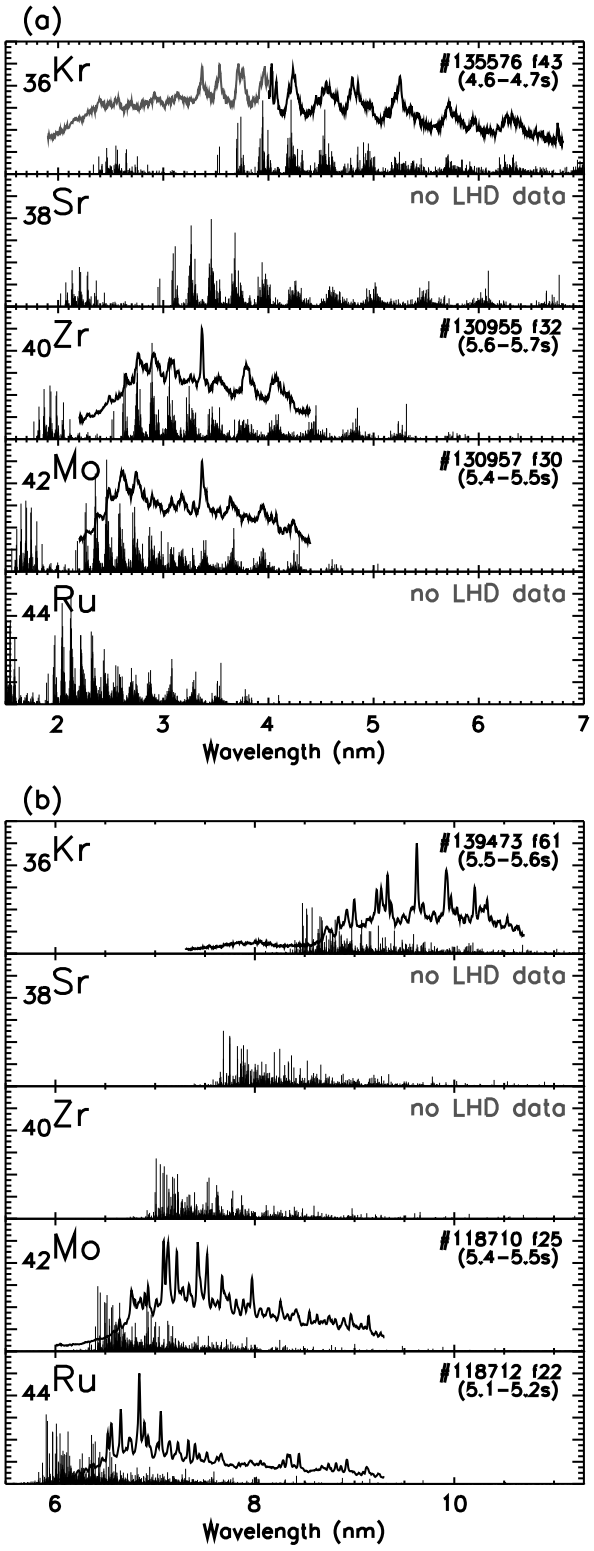

FIGURE 3 The measured spectra of M-shell ions of even Z elements from krypton to ruthenium for (a) n=3–4 and (b) n=3–3 transitions. The calculated line strengths are superposed with numerous vertical bars. Note that the experimental data for some cases (denoted by "no LHD data") have not been measured yet.

features are observed depending on the plasma temperature, which leads to some new experimental identifications of the spectral lines from lanthanide ions. The theoretical wavelengths are in good agreement with the measurements for $\Delta n \neq 0$ transitions, while they are systematically blue-shifted for $\Delta n = 0$ transitions associated with inner-subshell excited configurations. For the isolated spectral lines, more than 30 lines from ions with simple configurations have been identified so far, some of which are listed in our previous papers [4, 5, 6, 7]. Further line identifications are expected by constructing collisional radiative models or comparing with experimental data in other light sources.

Acknowledgments

The authors acknowledge the members of the LHD experiment group for their continuing support. This work was partially supported by JSPS KAKENHI Grant Numbers 15H03759 and 15H04234. This work was partially carried out under the auspices of the NIFS-collaboration research program (NIFS18KLPF062, NIFS17KLPH028).

References

[1] M. Finkenthal, et al., *Phys. Scr.* **1990**, *41*, 445.

[2] K. B. Fournier, et al., *Astrophys. J.* **2001**, *561*, 1144.

[3] T. Watanabe, et al., *Astrophys. J.* **2017**, *842*, 12.

[4] C. Suzuki, et al., *J. Phys. B: At. Mol. Opt. Phys.* **2012**, *45*, 135002.

[5] C. Suzuki, et al., *Plasma Phys. Control. Fusion* **2017**, *59*, 014009.

[6] C. Suzuki, F. Koike, I. Murakami, N. Tamura, and S. Sudo, *Atoms* **2018**, *6*, 24.

[7] C. Suzuki, et al., *J. Phys. B: At. Mol. Opt. Phys.* **2015**, *48*, 144012.

[8] S. Sudo, et al., *Plasma Phys. Control. Fusion* **2002**, *44*, 129.

[9] S. Sudo and N. Tamura, *Rev. Sci. Instrum.* **2012**, *83*, 023503.

[10] K. Narihara, et al., *Rev. Sci. Instrum.* **2001**, *72*, 1122.

[11] I. Yamada, et al., *Rev. Sci. Instrum.* **2010**, *81*, 10D522.

[12] J. L. Schwob, et al., *Rev. Sci. Instrum.* **1987**, *58*, 1601.

[13] C. Suzuki, et al., *Phys. Scr.* **2014**, *89*, 114009.

[14] G. O'Sullivan, et al., *Phys. Scr.* **2015**, *90*, 054002.

[15] G. O'Sullivan, et al., *J. Phys. B: At. Mol. Opt. Phys.* **2015**, *48*, 144025.

[16] J. Bauche, et al., *Phys. Scr.* **1988**, *37*, 659.

[17] H. Ohashi, et al., *Appl. Phys. Lett.* **2014**, *104*, 234107.

[18] M. F. Gu, *Can. J. Phys.* **2008**, *86*, 675.

[19] I. Murakami, et al., *Nucl. Fusion* **2015**, *55*, 093016.